Contribution from the Department of Chemistry,
University of Virginia, Charlottesville, Virginia 22901

# Carbon-Rich Metallacarboranes. 14.[1] Synthesis and Structure of Mixed-Ligand Cobalt and Iron Complexes Derived from $(C_2H_5)_4C_4B_8H_8^{2-}$ and $(C_2H_5)_2C_2B_4H_5^-$

ZHU-TING WANG,[2] EKK SINN, and RUSSELL N. GRIMES*

*Received June 26, 1984*

The preparation of metallacarboranes having $Et_4C_4B_8H_8^{2-}$ and $Et_2C_2B_4H_4^{2-}$ ligands bound to a common metal center was explored via reactions of $Et_4C_4B_8H_8^{2-}$ ion with $CoCl_2$ or $FeCl_2$ in tetrahydrofuran followed by addition of $Et_2C_2B_4H_5^-$. In the cobalt reaction the main products were purple $(Et_2C_2B_4H_4)Co(Et_4C_4B_8H_7OC_4H_8)$ (**6a**) and red-brown $(Et_2C_2B_4H_3)Co(EtC_4B_8H_6OC_4H_8)$ (**7**) with small amounts of $(Et_4C_4B_8H_7)_2CoH$ (**4b**), $(Et_4C_4B_8H_7)_2Co_2$ (**2b**), $(Et_4C_4B_8H_8)_2CoH(OC_4H_8)$ (**3b**), and $Et_6C_6B_{12}H_{12}$ (**8**). The corresponding iron reaction gave primarily red $(Et_2C_2B_3H_4)Fe^{III}H(Et_4C_4B_8H_7)$ (**11**), with minor products $(Et_2C_2B_4H_4)Fe^{III}(Et_4C_4B_8H_8OC_4H_8)$ (**9a,b**) and $(Et_2C_2B_4H_3)Fe^{II}H_2(Et_4C_4B_8H_7)$ (**10**). From spectroscopic evidence, **4b**, **7**, **10**, and **11** are proposed to have direct interligand bonds. An X-ray crystallographic study of **6a** confirmed the presence of *closo*-$CoC_2B_4$ and *nido*-$CoC_4B_8$ cages joined at a common cobalt vertex, with a THF substituent on the larger cage. The 13-vertex $CoC_4B_8$ system has the shape of a 14-vertex closo polyhedron (bicapped hexagonal antiprism) with an equatorial vertex missing and, except for the metal location, is analogous to the structure reported earlier for $[(C_6H_5)_2PCH_2]_2NiMe_4C_4B_8H_8$. Both cage systems in the molecule conform to the skeletal electron-counting rules for polyhedral cages. Crystal data: $[(C_2H_5)_2C_2B_4H_4]Co[(C_2H_5)_4C_4B_8H_7OC_4H_8]$, $M_r = 518$, space group $P2_1/c$, $a = 11.418$ (5) Å, $b = 14.639$ (3) Å, $c = 17.487$ (8) Å, $\beta = 100.74$ (3)°, $V = 2872$ Å$^3$, $Z = 4$, $R = 0.057$ for 2013 reflections having $F_o^2 > 3\sigma(F_o^2)$.

## Introduction

As we report in the accompanying paper,[1] a number of structurally varied bis(carboranyl)metal complexes, in some of which the two ligands appear to be directly linked, can be obtained from $CoCl_2$ and the $Et_4C_4B_8H_8^{2-}$ ion in tetrahydrofuran (THF) solution. A logical extension of this study would be the construction of mixed-ligand complexes in which the $Et_4C_4B_8H_8^{2-}$ ligand and the readily accessible $Et_2C_2B_4H_4^{2-}$ unit are coordinated to a common metal center. Such species conceivably could be induced to undergo oxidative ligand fusion[3] to give supra-icosahedral metallacarboranes such as $Et_6C_6B_{12}H_{12}$, a hypothetical 18-vertex system. Indeed, when one considers the large steric bulk of the $Et_4C_4B_8H_8^{2-}$ ion, fusion of a $C_4B_8$ with a $C_2B_4$ ligand appears more likely than does fusion of two $C_4B_8$ cages. This is borne out, on the one hand by the extreme facility with which $(C_2B_4)_2M$ complexes fuse to give $C_4B_8$ products[3] and on the other by the high oxidative stability of $(C_4B_8)_2Co$ complexes[1] and their failure, thus far, to exhibit fusion. We do not suggest that steric considerations are the only ones involved, but it is reasonable to assume that they play a large role in fusion chemistry.

The synthesis of mixed-ligand complexes is frequently complicated by differences in reactivity of the ligands toward the metal ion.[4] Optimization of yields in such circumstances may require extensive fine tuning of reaction conditions. In the present study this was not done, as the objective was to obtain quantities of representative mixed-ligand species sufficient for structural and chemical characterization.

## Results and Discussion

**Reaction of $Et_4C_4B_8H_8^{2-}$, $CoCl_2$, and $Et_2C_2B_4H_5^-$.** Since the $R_2C_2B_4H_5^-$ ions (R = H, alkyl) rapidly complex first-row transition-metal ions to form $(R_2C_2B_4H_4)_2MH_x$ products,[3a,b] while the $R_4C_4B_8H_8^{2-}$ ions react somewhat more slowly, the disodium salt of the latter ion (R = ethyl) was first treated for 2 h with $CoCl_2$ and subsequently allowed to react with $Na^+Et_2C_2B_4H_5^-$ in THF. This procedure gave a black product mixture, which on workup in air and chromatography on silica afforded a multitude of compounds (over 20 bands), most of which were in very low yields and were not isolated. The major isolable products are shown in Scheme I. The products (labeled according to the scheme of the preceding paper,[1] with the addition of new structural classes 6 and 7) include several species of the desired mixed-ligand type and others that contain only $C_4B_8$ ligands. Compound **6a** was initially characterized from its mass spectrum, whose high-mass cutoff at $m/e$ 521 ($^{13}C$ peak) and parent group profile match the formula given, its $^{11}B$ NMR spectrum (Table I), which indicates an absence of molecular symmetry planes or axes, and its infrared spectrum (Table II). The presence of a THF substituent was deduced from the intense grouping at $m/e$ 448 in the mass spectrum (corresponding to the loss of an $OC_4H_8$ fragment) as well as the singlet resonance in the proton-coupled $^{11}B$ NMR spectrum. In order to establish the precise geometry of this prototype $(C_2B_4)M(C_4B_8)$ complex, an X-ray structural analysis was undertaken and is reported below. The structure of **6a** contains separate, nonlinked $C_2B_4$ and $C_4B_8$ ligands, represented schematically as class 6 in Figure 1.

**Scheme I**

$$Et_4C_4B_8H_8^{2-} \xrightarrow[(2)\ Et_2C_2B_4H_5^-]{(1)\ CoCl_2}$$

$(Et_2C_2B_4H_4)Co(Et_4C_4B_8H_7OC_4H_8)$ (**6a**) (purple, 8%)

$(Et_2C_2B_4H_3)Co(Et_4C_4B_8H_6OC_4H_8)$ (**7**) (red-brown, 13%)

$(Et_4C_4B_8H_7)_2Co_2$ (**2b**) (golden, 4%)

$(Et_4C_4B_8H_8)CoH(Et_4C_4B_8H_8OC_4H_8)$ (**3b**) (green, 1%)

$(Et_4C_4B_8H_7)_2CoH$ (**4b**) (orange, 5%)

$Et_6C_6B_{12}H_{12}$(?) (**8**) (colorless, 1%)

Complex **7** exhibits a mass spectrum with a cutoff at $m/e$ 519, two units lower, than **6a**, although the intensity pattern in the parent region is similar; thus **7** appears to have two fewer hydrogen atoms than **6a** and on this basis is formulated as given above and assigned a linked-cage structure of the class 7 type (Figure 1). Intense groupings with local cutoffs at $m/e$ 423 and 332 correspond to net loss of BH + $B(OC_4H_8)$ and of $Co(Et_2C_2B_4H)$, respectively. The $^{11}B$ NMR spectrum of **7** is basically uniformative, with the resonances compressed into a small range of chemical shifts (Table I).

The orange product **4b**, with a small spectral cutoff at $m/e$ 579 and a pattern of intensities corresponding to that calculated for a $C_{24}B_{16}Co$ species, is proposed to have a B–B-linked $(C_4B_8)_2Co$ structure of the class 4 type as defined in Figure 1 of the preceding paper.[1] This assignment is supported by the presence of a singlet in the proton-coupled $^{11}B$ NMR spectrum, attributed to equivalent boron atoms involved in the direct interligand link and hence lacking attached hydrogens. Compound **2b** was identified spectroscopically as the same linked dicobalt species obtained in the $Et_4C_4B_8H_8^{2-}$–$CoCl_2$ reaction,[1] and the trace product **8** is tentatively assigned the formula $Et_6C_6B_{12}H_{12}$ from its mass spectrum. This

(1) Part 13: Wang, Z-T.; Sinn, E.; Grimes, R. N. *Inorg. Chem.* preceding paper in this issue.
(2) Visiting scholar from the Institute of Chemistry, Academica Sinica, Beijing, China, 1981–1983.
(3) (a) Grimes, R. N. *Adv. Inorg. Chem. Radiochem.* **1983**, *26*, 55 and references therein. (b) Maxwell, W. M.; Miller, V. R.; Grimes, R. N. *Inorg. Chem.* **1976**, *15*, 1343. (c) Venable, T. L.; Maynard, R. B.; Grimes, R. N. *J. Am. Chem. Soc.* **1984**, *106*, 6187.
(4) (a) Hosmane, N. S.; Grimes, R. N. *Inorg. Chem.* **1980**, *19*, 3482. (b) Borodinsky, L.; Grimes, R. N. *Inorg. Chem.* **1982**, *21*, 1921.

0020-1669/85/1324-0834$01.50/0 

Table I. 115.8-MHz $^{11}$B FT NMR Data

| compd | solvent[a] | δ (*J*, Hz)[b,c] | rel area |
|---|---|---|---|
| $(Et_4C_4B_8H_8)_2(OC_4H_8)CoH$ (**3b**) | D | 35.6 (s), 8.9 (126), 1.9 (168), −6.7 (149), −8.5,[d] −15.6 (152), −25.5 (159), −43.7 (149) | equal areas |
| $(Et_4C_4B_8H_7)_2CoH$ (**4b**) | D | 33.6 (s), 19.8 (107), 8.8 (144), 1.7 (165), [−6.9 (150), −8.8[d]],[e] −15.7 (157), [−23.6,[d] −25.4 (148)],[e] −43.9 (147) | 1:1:1:1:7:1:3:1 |
| $(Et_2C_2B_4H_4)Co(Et_4C_4B_8H_7OC_4H_8)$ (**6a**) | D | 11.8,[d,e] 9.2 (s),[e] 6.1,[d,e] 1.4 (131), −3.8 (126), −12.0,[d] −17.8 (130), −23.1 (163), −24.5 (137), −32.3 (128) | 1:2:2:1:1:1:1:1:1:1 |
| $(Et_2C_2B_4H_3)Co(Et_4C_4B_8H_6OC_4H_8)$ (**7**) | A | [−2.9,[d] −7.6 (114)],[e] −22.5 (133) | 9:3 |
| $(Et_2C_2B_4H_4)Fe(Et_4C_4B_8H_8OC_4H_8)$ (**9b**)[f] | C | 63.0, ~−3, −71.7, −194.3 | ~3:4:2:0.2 |
| $(Et_2C_2B_4H_3)FeH_2(Et_4C_4B_8H_7)$ (**10**)[g] | C | 33.1 (138), 23.1 (154), 19.1 (119), 16.8 (177), [11.4 (s), 10.7[d]],[e] −0.4 (110), −5.1 (156), −9.1 (139), −11.5 (165), −14.4 (139), −21.5 (157), −26.0 (147) | 2:2:2:1:4:4:2:1:2:2:1:1 |
| $(Et_2C_2B_3H_4)FeH(Et_4C_4B_8H_7)$ (**11**)[f] | A | 41.0, −14.3, −47.8 | ~2:2:1 |

[a] Legend: A = acetone; C = $CH_2Cl_2$; D = $CDCl_3$. [b] Legend: s = singlet (no B–H coupling). [c] Chemical shifts relative to $BF_3{\cdot}O(C_2H_5)_2$. [d] *J* value not measurable. [e] Superimposed or overlapped peaks. [f] Paramagnetic compound; broad peaks, B–H coupling not observed. [g] Mixture of isomers.

Table II. Infrared Absorptions ($cm^{-1}$)[a,b]

**3b** 2980 vs, 2940 s, 2890 m, 2525 s, 1730 m, 1650 w, br, 1460 m, 1375 s, 1348 w, 1330 w, 1270 w, 1255 w, 1160 m, 1130 m, 1080 m, 1040 w, 990 w, 950 s, 900 w, 860 w

**4b** 2980 s, 2940 s, 2880 s, 2570 vs, 2360 w, 1650 w, br, 1475 w, 1455 s, 1380 s, 1310 m, 1235 w, 1170 w, 990 m, 940 m, 920 m, 680 s

**6a** 3655 m, 2980 vs, 2945 vs, 2890 s, 2580 vs, 1735 m, 1465 s, 1385 s, 1310 s, br, 1280 w, 1190 w, 1140 w, br, 940 w, 925 m

**7** 2980 s, 2950 s, 2890 m, 2580 m, 1720 s, 1550 m, br, 1450 m, br, 1365 s, 1270 m, 1220 s, 1100 w, 1010 m, br

**9a** 3020 vs, 2990 vs, 2950 vs, 2900 m, 2800 w, 2580 vs, 2160 w, 1730 vs, 1710 vs, 1430 vs, br, 1360 vs, br, 1225 vs, 1095 s, 910 s

**11** 2995 s, 2955 s, 2900 m, 2560 s, 2380 w, 1725 m, 1520 w, 1470 m, 1390 m, 1340 w, br, 1245 m, 1200 m, 940 w, br

[a] Key: vs = very strong; s = strong; m = medium; w = weak; br = broad. [b] $CCl_4$ solution vs. $CCl_4$.

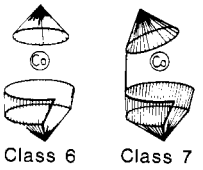


**Figure 1.** Schematic representations of structure types of $(C_2B_4)Co(C_4B_8)$ complexes (For classes 1–5, see Figure 1 of preceding paper[1]). The small ligand is $Et_2C_2B_4H_4^{2-}$; the large ligand is $Et_4C_4B_8H_8^{2-}$.

composition suggests an origin via oxidative fusion of $Et_2C_2B_4H_4^{2-}$ and $Et_4C_4B_8H_8^{2-}$ ligands, but this species is at present not well characterized.

The green complex **3b** is of interest in that its high-resolution (115.8-MHz) $^{11}$B NMR spectrum is identical within experimental error to that of **4a**, a demonstrably different complex characterized as $(Et_4C_4B_8H_7)_2CoH$, which was isolated from the $Et_4C_4B_8H_8^{2-}$–$CoCl_2$ reaction described elsewhere.[1] These compounds exhibit quite distinct infrared and mass spectra and are clearly not isomers. The mass spectrum of **3b** cuts off at 74 mass units higher than **4a** and indicates the presence of a THF ligand as well as two more hydrogens than **4a**. A probable solution to this rather intriguing structural problem is given by the two-dimensional (2D) $^{11}$B spectrum[5] of **3b**, which matches that of **4a**

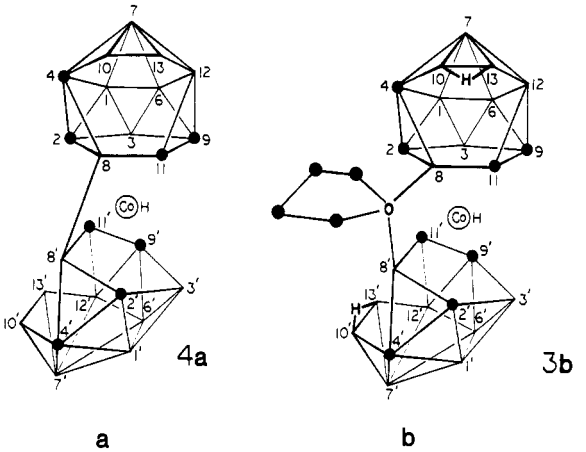


**Figure 2.** Proposed structures of (a) **4a** and (b) **3b**, based on two-dimensional $^{11}$B NMR data (see text). Skeletal and THF carbon atoms are shown as solid circles.

(see Figure 4 of preceding paper) except that the B(13)–B(12) and B(13)–B(10) cross peaks, which are present in **4a**, are absent in **3b**. Since the one-dimensional spectra are, as noted, essentially identical, it is clear that the cage structures of the two complexes are the same; consequently, the "missing" cross peaks in **3b** suggest that the B(13)–B(12) and B(13)–B(10) edges contain B–H–B bridges. Earlier work has shown that hydrogen-bridged boron nuclei usually do not exhibit scalar coupling and hence fail to give cross peaks.[5] The fact that these particular boron atoms all lie on the rims of the open faces in the proposed structure of **4a** (Figure 2a) lends further plausibility to this idea. Since both **3b** and **4a** contain two equivalent carborane ligands, it would appear that two B–H–B bridges per ligand, or a total of four, are required; yet **3b** has only two "extra" hydrogens. Nevertheless, tautomerism of a proton between the B(13)–B(12) and B(13)–B(10) edges, and of a second proton between the equivalent B(13′)–B(12′) and B(13′)–B(10′) edges (Figure 2b), could effectively eliminate the corresponding cross peaks and account for the 2D spectrum of **3b**. Inasmuch as the B(8) resonance is not shifted in **3b** relative to its position in **4a**, it may be that the THF substituent in **3b** is fluxional in solution, spending only part of the time attached to B(8) (and B(8′)) and resulting in a time-averaged 1D spectrum.

**Attempted Oxidative Fusion of 6a.** The mixed-ligand complex **6a**, like most complexes derived from $R_4C_4B_8H_8^{2-}$ ligands,[1,3a] is stable toward air oxidation. In an effort to induce ligand fusion, **6a** was exposed to other oxidants, including $FeCl_3$, which resulted

(5) Venable, T. L.; Hutton, W. C.; Grimes, R. N. *J. Am. Chem. Soc.* **1984**, *106*, 29.

Table III. Experimental Parameters and Crystal Data

| | | | |
|---|---|---|---|
| space group | $P2_1/c$ | $D$(calcd), g cm$^{-3}$ | 1.20 |
| $a$, Å | 11.418 (5) | $\mu$, cm$^{-1}$ | 6.4 |
| $b$, Å | 14.639 (3) | esd unit wt | 1.93 |
| $c$, Å | 17.487 (8) | $Z$ | 4 |
| $\beta$, deg | 100.74 (3) | radiation | Mo K$\alpha$ ($\lambda$ = 0.7107 Å) |
| $V$, Å$^3$ | 2872 | | |

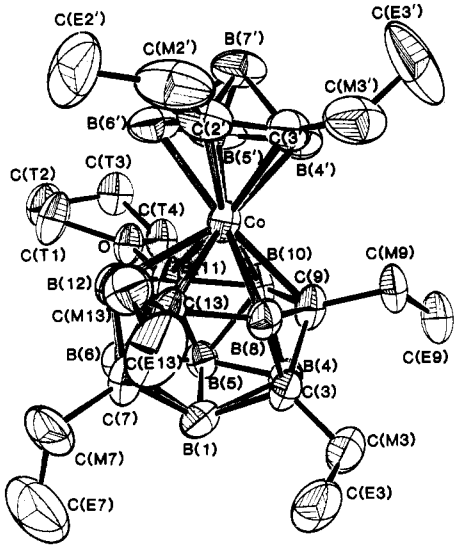


**Figure 3.** ORTEP view of the molecular structure of $(Et_2C_2B_4H_4)Co(Et_4C_4B_8H_7OC_4H_8)$ (**6a**), with hydrogen atoms omitted for clarity.

in decomposition to noncharacterizable products. Treatment of **6a** with iodine produced a low yield of a derivative identified from its mass spectrum as $(Et_2C_2B_4H_4)Co(Et_4C_4B_8H_8)(OC_4H_8)I$ (**6b**), which indicates net addition of an HI unit to **6a**. No evidence of a fused carborane product was detected.

**Reaction of $Et_4C_4B_8H_8^{2-}$, $FeCl_2$, and $Et_2C_2B_4H_5^-$.** In a two-step sequence similar to that employed for the corresponding $CoCl_2$ reaction described above, the $Et_4C_4B_8H_8^{2-}$ dianion and $FeCl_2$ were allowed to react for 2 h at 25 °C in THF, forming a dark red solution, after which the $Et_2C_2B_4H_5^-$ ion was introduced and the reaction continued overnight. This generated several characterizable mixed-ligand species, including isomers of $(Et_2C_2B_4H_4)Fe(Et_4C_4B_8H_8OC_4H_8)$ (**9a,b**), a probable linked-cage complex, $(Et_2C_2B_4H_3)FeH_2(Et_4C_4B_8H_7)$ (**10**), and the major product, $(Et_2C_2B_3H_4)FeH(Et_4C_4B_8H_7)$ (**11**). Complexes **9a,b** and **11** are evidently paramagnetic, from their NMR spectra, and are presumed to contain Fe(III); **10** is diamagnetic and is formulated as an iron(II) species. The $^{11}B$ spectrum of **10** (Table I) cannot arise from a single species and hence is interpreted as a mixture of isomers, which were not separated. These $(C_2B_4)Fe(C_4B_8)$ complexes are less air stable than their cobalt counterparts but have shown no tendency to undergo oxidative fusion.

**Crystallographic Study of $(Et_2C_2B_4H_4)Co(Et_4C_4B_8H_7OC_4H_8)$ (6a).** The unit cell and data collection parameters, atomic coordinates, bond distances, and selected angles are given in Tables III–VI, and an ORTEP view of the molecule is presented in Figure 3. As anticipated, the complex consists of closo 7-vertex $CoC_2B_4$ and nido 13-vertex $CoC_4B_8$ cages with the metal occupying a common vertex. The smaller polyhedron exhibits normal bond distances and angles for 7-vertex $MC_2B_4$ closo systems,[6] with a typically short carbon–carbon (C(2')–C(3')) length of 1.451 (8) Å, suggesting localized multiple bonding in that region. One unusual finding is that the cobalt is slightly closer to the three boron atoms of the $C_2B_3$ bonding face than it is to the two carbons, the difference between ⟨Co–B⟩ and ⟨Co–C⟩ amounting to 0.033 Å or about 5 standard deviations. This is contrary to observations in previously determined $CoC_2B_4$ and $FeC_2B_4$ closo systems,[6]

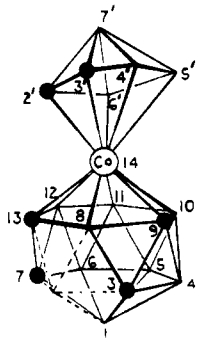


**Figure 4.** Cage geometry in **6a**, depicting the 13-vertex $CoC_4B_8$ unit as a fragment of a bicapped hexagonal antiprism. The missing vertex (2) is shown by dashed lines. Framework carbon atoms are represented as solid circles; other vertices are boron.

where the metal–carbon distances are typically smaller by about 0.1 Å. There is, however, a precedent in the gallium analogue $CH_3GaC_2B_4H_6$,[7] and it is clear that the nature of the exo polyhedral ligand(s) on the metal atom can influence the bonding within the cage. Thus, in the species $(\eta^8\text{-}C_8H_8)MEt_2C_2B_4H_4$ (M = V, Ti), the metal is very nearly equidistant from the members of the $C_2B_3$ bonding face.[6] In the present case the interaction of cobalt with the formal $Et_4C_4B_8H_8^{2-}$ ligand may serve to weaken selectively the Co–C bonding (in the $CoC_2B_4$ cage), perhaps reflecting slightly greater ionic character in the Co–C vs. the Co–B interactions.

The $CoC_4B_8$ cluster can be described as a 13-vertex nido framework that is formally derived from a closo 14-vertex cage (bicapped hexagonal antiprism) by removal of an equatorial vertex as illustrated in Figure 4. The nido geometry (although not the specific arrangement of hetero atoms) is predicted by the polyhedral skeletal electron counting theory (PSEPT)[8] if cobalt in this case is assumed to contribute one electron to skeletal bonding.[9] With the usual contributions of three and two electrons from C–$C_2H_5$ and BH units, respectively, plus three from the B–$OC_4H_8$ unit, there are 30 framework bonding electrons; for a 13-vertex system this predicts nido geometry, as observed. However, in principle two kinds of nido fragments can be derived from a bicapped hexagonal antiprism, via removal of a six-coordinate (apical) vertex or a five-coordinate (equatorial) vertex. In **6a** the observed structure, which is of the first type, places three of the four cage carbon atoms in low-coordinate positions on the five-membered open face. The alternate geometry could be formed by moving B(1) up into the open face, thereby creating a new, six-membered open face that, however, would contain only two carbons and hence is less attractive.[3a] Another argument against this latter arrangement is that it appears to have no precedent in metallacarborane chemistry; planar open faces larger than five members are avoided in favor of alternative geometries.

The nickelacarborane $[(C_6H_5)_2PCh_2]_2NiMe_4C_4B_8H_8$, reported earlier,[10] has a 13-vertex *nido*-$MC_4B_8$ cage structure analogous to that of **6a** and is the only previously confirmed example of this geometry. There is, however, one difference: in the nickel complex the metal is on the five-membered open face (in vertex 1), while in **6a** the metal occupies an off-facial vertex (14). (In the coding system introduced earlier[3a] the nickel species is a *5-4445*(5) system while **6a** is 6-*4445*(5)). Since all four cage carbons are located in corresponding vertices (3, 7, 9, and 13) in the two structures,

(6) Swisher, R. G.; Sinn, E.; Grimes, R. N. *Organometallics* **1984**, *3*, 599 and references therein.

(7) Grimes, R. N.; Rademaker, W. J.; Denniston, M. L.; Bryan, R. F.; Green, P. T. *J. Am. Chem. Soc.* **1972**, *94*, 1865.

(8) (a) Wade, K. *Adv. Inorg. Chem. Radiochem.* **1976**, *18*, 1. (b) Rudolph, R. W. *Acc. Chem. Res.* **1976**, *9*, 446. (c) Mingos, D. M. P. *Nature (London), Phys. Sci.* **1972**, *236*, 99. (d) O'Neill, M. E.; Wade, K. In "Metal Interactions with Boron Clusters"; Grimes, R. N.; Ed.; Plenum Press: New York, 1982; Chapter 1, and references therein.

(9) Assigning six of cobalt's nine valence electrons to nonbonding orbitals[8] leaves three available for the bonding MOs in the two cluster systems; of these, two are required to satisfy the quota of 16 ($2n$ + 2) for the $CoC_2B_4$ cage.[8]

(10) Grimes, R. N.; Sinn, E.; Pipal, J. R. *Inorg. Chem.* **1980**, *19*, 2087.

Table IV. Positional Parameters for $[(C_2H_5)_2C_2B_4H_4]Co[(C_2H_5)_4C_4B_8H_7OC_4H_8]$ (6a)

| atom | x | y | z | atom | x | y | z |
|---|---|---|---|---|---|---|---|
| Co | 0.1822 (1) | 0.20144 (7) | 0.33553 (6) | H(T42) | 0.342 (6) | −0.058 (4) | 0.477 (4) |
| O | 0.2661 (5) | 0.0622 (3) | 0.4783 (3) | H(1) | 0.595 (5) | 0.203 (4) | 0.371 (3) |
| C(T1) | 0.2398 (9) | 0.0885 (6) | 0.5552 (5) | H(M31) | 0.442 (5) | 0.250 (4) | 0.164 (3) |
| C(T2) | 0.2322 (8) | 0.0017 (6) | 0.5957 (5) | H(M32) | 0.540 (6) | 0.207 (5) | 0.206 (4) |
| C(T3) | 0.1989 (8) | −0.0680 (5) | 0.5327 (5) | H(E31) | 0.611 (6) | 0.353 (5) | 0.178 (4) |
| C(T4) | 0.2622 (8) | −0.0381 (5) | 0.4691 (4) | H(E32) | 0.604 (7) | 0.344 (6) | 0.266 (5) |
| C(3) | 0.4269 (7) | 0.2251 (5) | 0.2691 (4) | H(E33) | 0.502 (7) | 0.388 (6) | 0.213 (5) |
| C(M3) | 0.4952 (8) | 0.2482 (6) | 0.2040 (5) | H(4) | 0.470 (6) | 0.066 (4) | 0.258 (4) |
| C(E3) | 0.5564 (10) | 0.3369 (7) | 0.2169 (5) | H(5) | 0.485 (6) | 0.028 (5) | 0.413 (4) |
| C(7) | 0.4369 (7) | 0.2838 (5) | 0.4167 (4) | H(6) | 0.506 (6) | 0.171 (4) | 0.513 (4) |
| C(M7) | 0.5117 (9) | 0.3560 (6) | 0.4693 (6) | H(M71) | 0.476 (7) | 0.364 (5) | 0.513 (5) |
| C(E7) | 0.6322 (13) | 0.3448 (9) | 0.4887 (9) | H(M72) | 0.504 (8) | 0.417 (6) | 0.444 (5) |
| C(9) | 0.3015 (7) | 0.1665 (5) | 0.2529 (4) | H(E71) | 0.670 (6) | 0.389 (5) | 0.523 (4) |
| C(M9) | 0.2513 (8) | 0.1449 (5) | 0.1671 (4) | H(E72) | 0.676 (8) | 0.352 (6) | 0.445 (5) |
| C(E9) | 0.3006 (10) | 0.0650 (6) | 0.1302 (5) | H(E73) | 0.655 (7) | 0.290 (5) | 0.505 (4) |
| C(13) | 0.3159 (7) | 0.3147 (5) | 0.3647 (4) | H(8) | 0.277 (5) | 0.324 (4) | 0.234 (4) |
| C(M13) | 0.2763 (8) | 0.4129 (5) | 0.3743 (5) | H(M91) | 0.256 (6) | 0.200 (5) | 0.146 (4) |
| C(E13) | 0.3333 (11) | 0.4847 (6) | 0.3304 (6) | H(M92) | 0.177 (5) | 0.133 (4) | 0.161 (3) |
| C(2′) | 0.0219 (8) | 0.2817 (6) | 0.3328 (5) | H(E91) | 0.384 (5) | 0.069 (4) | 0.130 (3) |
| C(M2′) | −0.0205 (10) | 0.3800 (7) | 0.3348 (7) | H(E92) | 0.256 (7) | 0.057 (5) | 0.083 (4) |
| C(E2′) | −0.0223 (12) | 0.4155 (9) | 0.4142 (8) | H(E93) | 0.286 (6) | 0.010 (5) | 0.159 (4) |
| C(3′) | 0.0204 (8) | 0.2368 (6) | 0.2586 (5) | H(10) | 0.254 (5) | 0.016 (4) | 0.304 (3) |
| C(M3′) | −0.0139 (9) | 0.2884 (8) | 0.1820 (6) | H(12) | 0.276 (6) | 0.272 (4) | 0.489 (4) |
| C(E3′) | −0.1126 (16) | 0.2469 (11) | 0.1281 (8) | H(M131) | 0.197 (5) | 0.418 (4) | 0.363 (3) |
| B(1) | 0.5010 (8) | 0.2076 (7) | 0.3633 (5) | H(M132) | 0.294 (6) | 0.432 (5) | 0.429 (4) |
| B(4) | 0.4328 (9) | 0.1154 (6) | 0.2924 (5) | H(E131) | 0.304 (7) | 0.549 (5) | 0.326 (5) |
| B(5) | 0.4337 (9) | 0.0938 (6) | 0.3887 (5) | H(E132) | 0.328 (8) | 0.465 (6) | 0.284 (5) |
| B(6) | 0.4377 (9) | 0.1822 (6) | 0.4547 (5) | H(E133) | 0.424 (8) | 0.491 (7) | 0.354 (5) |
| B(8) | 0.3114 (8) | 0.2799 (6) | 0.2777 (5) | H(M2′1) | 0.025 (7) | 0.420 (5) | 0.306 (4) |
| B(10) | 0.2951 (9) | 0.0875 (6) | 0.3226 (5) | H(M2′2) | −0.099 (6) | 0.380 (5) | 0.303 (4) |
| B(11) | 0.3028 (9) | 0.1269 (6) | 0.4188 (5) | H(E2′1) | −0.052 (7) | 0.477 (5) | 0.415 (4) |
| B(12) | 0.3070 (9) | 0.2471 (6) | 0.4401 (5) | H(E2′2) | 0.055 (7) | 0.412 (6) | 0.444 (5) |
| B(4′) | 0.0360 (10) | 0.1328 (8) | 0.2675 (6) | H(E2′3) | −0.082 (8) | 0.371 (6) | 0.443 (5) |
| B(5′) | 0.0486 (10) | 0.1098 (8) | 0.3616 (7) | H(M3′1) | 0.040 (6) | 0.299 (5) | 0.155 (4) |
| B(6′) | 0.0458 (9) | 0.2124 (8) | 0.4007 (6) | H(M3′2) | −0.032 (8) | 0.354 (6) | 0.198 (5) |
| B(7′) | −0.0639 (9) | 0.1815 (8) | 0.3212 (6) | H(E3′1) | −0.153 (7) | 0.297 (5) | 0.079 (4) |
| H(T11) | 0.183 (7) | 0.133 (5) | 0.545 (4) | H(E3′2) | −0.184 (8) | 0.229 (6) | 0.155 (5) |
| H(T12) | 0.297 (6) | 0.129 (5) | 0.579 (4) | H(E3′3) | −0.090 (8) | 0.186 (6) | 0.108 (5) |
| H(T21) | 0.180 (6) | 0.003 (5) | 0.627 (4) | H(4′) | 0.026 (6) | 0.064 (5) | 0.221 (4) |
| H(T22) | 0.306 (6) | −0.014 (5) | 0.624 (4) | H(5′) | 0.050 (6) | 0.039 (5) | 0.386 (4) |
| H(T31) | 0.217 (6) | −0.128 (5) | 0.548 (4) | H(6′) | 0.043 (6) | 0.239 (5) | 0.456 (4) |
| H(T32) | 0.118 (6) | −0.066 (4) | 0.519 (4) | H(7′) | −0.154 (6) | 0.177 (5) | 0.310 (4) |
| H(T41) | 0.224 (6) | −0.053 (5) | 0.420 (4) | | | | |

it is probable that these species were formed from topologically equivalent $R_4C_4B_8H_8^{2-}$ ions, but with metal attack in the two cases taking place at different locations on the carborane framework.[3a,11] In these structures the skeletal carbon atoms are present as bonded pairs, reflecting the geometry of the neutral $R_4C_4B_8H_8$ carborane precursors.[3a,c] (Although reduction to the dianions involves structural changes,[11] available evidence indicates that the framework carbon–carbon bonds remain intact.)

A related chromium species, $(\eta^5\text{-}C_5H_5)CrEt_4C_4B_8H_8$, also has a 13-vertex nido structure,[12] but in this case the cage geometry is irregular and is not a fragment of a bicapped hexagonal antiprism, in contrast to **6a** and the nickel compound just cited. However, in common with **6a** the chromacarborane cage does have a CCBCB open face and the metal occupies a six-coordinate vertex (6-*3445*(5) geometry), further underlining some of the structural trends noted above and elsewhere.

The cobalt atom in **6a** is located 1.659 Å from the bonding face of the $C_2B_4$ ligand (C(2′)–C(3′)–B(3′)–B(4′)–B(5′)) and 1.369 Å from the plane calculated for the B(8)–C(9)–B(10)–B(11)–B(12)–C(13) array in the $C_4B_8$ ligand, to which cobalt is coordinated. These values are typical for first-row transition-metal interactions with five- and six-membered carborane faces, respectively. The two metal-bound faces are nearly planar, with maximum deviations of 0.027 and 0.044 Å from the calculated planes. These faces are slightly tilted (dihedral angle 10.9°) such that B(5′) and B(6′) are closest to the $C_4B_8$ ligand, but there are no interligand distances that could be considered bonding, the shortest being B(5′)–B(11) (2.899 (8) Å) (Table V).

The open face on the $CoC_4B_8$ cage is well-defined, with all transfacial distances clearly nonbonding. In conformity with trends noted previously,[3a] the carbon–carbon distance on the open face (1.573 (7) Å) is shorter than the nonfacial C(3)–C(9) bond length (1.648 (7) Å), which involves higher coordinate carbon atoms.

## Conclusions

This work together with earlier efforts[4] demonstrates that mixed-ligand metal–carborane and metal–borane complexes are accessible by straightforward synthetic methods, but the control of reaction conditions is critical. The products obtained in the present study proved unexpectedly resistant to ligand fusion via oxidation. Nevertheless, the observation of species with intercage links (suggestive of an early stage of fusion), and of a possible $C_6B_{12}$ system in small amounts, encourages the thought that efficient metal-promoted fusion of $C_2B_4$ and $C_4B_8$ units can be achieved. Relevant to this point, work in this laboratory[4a] has shown that an apparent supra-icosahedral carborane, $Me_4C_4B_{11}H_{11}$, can be obtained on oxidation of $(Me_2C_2B_4H_4)$-$FeH_2(Me_2C_2B_7H_7)$. Quite possibly the use of carborane ligands in which the substituents on carbon are $CH_3$ (or even H), rather than $C_2H_5$, tends to lower the steric barriers to fusion. That metal-promoted ligand fusion is a general phenomenon in boron cluster chemistry is clear from a number of studies,[13] including

(11) Grimes, R. N.; Pipal, J. R.; Sinn, E. *J. Am. Chem. Soc.* **1979**, *101*, 4172.
(12) Maynard, R. B.; Wang, Z.-T.; Sinn, E.; Grimes, R. N. *Inorg. Chem.* **1983**, *22*, 873. This complex was not the first nido 13-vertex metallacarborane as stated;[12] we overlooked $[(C_6H_5)_2PCH_2]_2NiEt_4C_4B_8H_8$.[10]
(13) Maynard, R. B.; Grimes, R. N. *J. Am. Chem. Soc.* **1982**, *104*, 5983 and references therein.

Table V. Interatomic Distances (Å) for **6a**

| | | | |
|---|---|---|---|
| Bond Distances for Non-Hydrogen Atoms | | | |
| Co-B(8) | 2.253 (6) | B(5)-B(11) | 1.744 (9) |
| Co-C(9) | 2.222 (5) | B(6)-C(7) | 1.628 (7) |
| Co-B(10) | 2.146 (6) | B(6)-B(11) | 1.750 (9) |
| Co-B(11) | 2.112 (7) | B(6)-B(12) | 1.747 (9) |
| Co-B(12) | 2.202 (6) | C(7)-C(M7) | 1.549 (7) |
| Co-C(13) | 2.247 (5) | C(7)-B(12) | 1.698 (8) |
| Co-C(2′) | 2.167 (6) | C(7)-C(13) | 1.573 (7) |
| Co-C(3′) | 2.136 (6) | C(M7)-C(E7) | 1.363 (11) |
| Co-B(4′) | 2.114 (7) | B(8)-C(9) | 1.715 (8) |
| Co-B(5′) | 2.144 (7) | B(8)-C(13) | 1.596 (7) |
| Co-B(6′) | 2.099 (6) | C(9)-C(M9) | 1.536 (7) |
| O-C(T1) | 1.481 (6) | C(9)-B(10) | 1.691 (7) |
| O-C(T4) | 1.478 (6) | C(M9)-C(E9) | 1.496 (8) |
| O-B(11) | 1.522 (7) | B(10)-B(11) | 1.765 (8) |
| C(T1)-C(T2) | 1.465 (8) | B(11)-B(12) | 1.797 (9) |
| C(T2)-C(T3) | 1.499 (8) | B(12)-C(13) | 1.667 (7) |
| C(T3)-C(T4) | 1.499 (7) | C(13)-C(M13) | 1.525 (7) |
| B(1)-C(3) | 1.726 (8) | C(M13)-C(E13) | 1.518 (8) |
| B(1)-B(4) | 1.900 (9) | C(2′)-C(M2′) | 1.521 (8) |
| B(1)-B(5) | 1.920 (9) | C(2′)-C(3′) | 1.451 (8) |
| B(1)-B(6) | 1.908 (8) | C(2′)-B(6′) | 1.547 (9) |
| B(1)-C(7) | 1.705 (8) | C(2′)-B(7′) | 1.754 (9) |
| C(3)-C(M3) | 1.533 (7) | C(M2′)-C(E2′) | 1.487 (10) |
| C(3)-B(4) | 1.655 (8) | C(3′)-C(M3′) | 1.524 (8) |
| C(3)-B(8) | 1.575 (8) | C(3′)-B(4′) | 1.537 (9) |
| C(3)-C(9) | 1.648 (7) | C(3′)-B(7′) | 1.781 (9) |
| C(M3)-C(E3) | 1.472 (8) | C(M3′)-C(E3′) | 1.459 (11) |
| B(4)-B(5) | 1.711 (8) | B(4′)-B(5′) | 1.660 (11) |
| B(4)-C(9) | 1.701 (9) | B(4′)-B(7′) | 1.757 (10) |
| B(4)-B(10) | 1.797 (9) | B(5′)-B(6′) | 1.653 (11) |
| B(5)-B(6) | 1.729 (8) | B(5′)-B(7′) | 1.707 (10) |
| B(5)-B(10) | 1.780 (9) | B(6′)-B(7′) | 1.748 (11) |
| Long Distances | | | |
| B(1)-B(8) | 2.616 (8) | B(11)-B(5′) | 2.899 (8) |
| B(1)-C(13) | 2.635 (9) | B(11)-B(6′) | 3.151 (8) |
| C(3)-C(7) | 2.703 (8) | B(12)-B(6′) | 2.977 (9) |
| C(3)-C(13) | 2.628 (8) | B(8)-C(3′) | 3.336 (8) |
| C(7)-B(8) | 2.583 (8) | B(12)-C(2′) | 3.478 (8) |
| C(9)-B(4′) | 3.128 (7) | C(13)-C(2′) | 3.334 (9) |
| B(10)-B(4′) | 3.010 (8) | B(8)-C(2′) | 3.611 (8) |
| B(10)-B(5′) | 3.035 (8) | C(13)-C(3′) | 3.713 (10) |
| Bond Distances Involving Hydrogen | | | |
| C(T1)-H(T11) | 0.913 (6) | C(M9)-H(M92) | 0.857 (6) |
| C(T1)-H(T12) | 0.921 (6) | C(E9)-H(E91) | 0.949 (8) |
| C(T2)-H(T21) | 0.885 (6) | C(E9)-H(E92) | 0.901 (6) |
| C(T2)-H(T22) | 0.924 (7) | C(E9)-H(E93) | 0.983 (7) |
| C(T3)-H(T31) | 0.935 (5) | B(10)-H(10) | 1.169 (6) |
| C(T3)-H(T32) | 0.913 (6) | B(12)-H(12) | 1.055 (6) |
| C(T4)-H(T41) | 0.909 (5) | C(M13)-H(M131) | 0.898 (6) |
| C(T4)-H(T42) | 0.939 (6) | C(M13)-H(M132) | 0.982 (6) |
| B(1)-H(1) | 1.063 (6) | C(E13)-H(E131) | 1.001 (6) |
| C(M3)-H(M31) | 0.846 (6) | C(E13)-H(E132) | 0.856 (7) |
| C(M3)-H(M32) | 0.787 (6) | C(E13)-H(E133) | 1.042 (8) |
| C(E3)-H(E31) | 1.026 (6) | C(M2′)-H(M2′1) | 0.971 (8) |
| C(E3)-H(E32) | 0.927 (7) | C(M2′)-H(M2′2) | 0.961 (7) |
| C(E3)-H(E33) | 0.965 (8) | C(E2′)-H(E2′1) | 0.965 (8) |
| B(4)-H(4) | 1.078 (6) | C(E2′)-H(E2′2) | 0.940 (10) |
| B(5)-H(5) | 1.169 (6) | C(E2′)-H(E2′3) | 1.128 (10) |
| B(6)-H(6) | 1.176 (6) | C(M3′)-H(M3′1) | 0.858 (7) |
| C(M7)-C(E7) | 1.363 (11) | C(M3′)-H(M3′2) | 1.030 (9) |
| C(M7)-H(M71) | 0.934 (7) | C(E3′)-H(E3′1) | 1.159 (9) |
| C(M7)-H(M72) | 0.988 (7) | C(E3′)-H(E3′2) | 1.045 (13) |
| C(E7)-H(E71) | 0.931 (8) | C(E3′)-H(E3′3) | 1.014 (13) |
| C(E7)-H(E72) | 0.997 (12) | B(4′)-H(4′) | 1.282 (7) |
| C(E7)-H(E73) | 0.876 (11) | B(5′)-H(5′) | 1.115 (7) |
| B(8)-H(8) | 1.022 (6) | B(6′)-H(6′) | 1.044 (7) |
| C(M9)-H(M91) | 0.888 (5) | B(7′)-H(7′) | 1.016 (7) |
| | ⟨B-H⟩ | 1.11 | |
| | ⟨C-H($C_2H_5$)⟩ | 0.97 | |

Table VI. Selected Bond Angles (deg) for **6a**

| | | | |
|---|---|---|---|
| B(8)-Co-B(4′) | 120.2 (3) | B(8)-C(9)-C(M9) | 116.1 (4) |
| C(9)-Co-B(4′) | 92.3 (3) | B(8)-C(9)-B(10) | 119.3 (4) |
| B(10)-Co-B(4′) | 89.9 (3) | C(M9)-C(9)-B(10) | 120.3 (4) |
| B(10)-Co-B(5′) | 90.1 (3) | C(9)-C(M9)-C(E9) | 118.7 (5) |
| B(10)-Co-B(6′) | 129.6 (3) | C(9)-B(10)-B(11) | 117.5 (4) |
| B(11)-Co-B(4′) | 119.2 (3) | Co-B(11)-O | 124.5 (4) |
| B(11)-Co-B(5′) | 85.9 (3) | O-B(11)-B(5) | 113.2 (5) |
| B(11)-Co-B(6′) | 96.9 (3) | O-B(11)-B(6) | 112.2 (4) |
| B(12)-Co-B(4′) | 158.8 (3) | O-B(11)-B(10) | 118.5 (5) |
| B(12)-Co-B(6′) | 87.5 (3) | O-B(11)-B(12) | 117.9 (4) |
| C(13)-Co-C(2′) | 98.1 (2) | B(10)-B(11)-B(12) | 120.8 (4) |
| C(13)-Co-C(3′) | 115.8 (2) | B(11)-B(12)-C(13) | 114.9 (4) |
| C(T1)-O-C(T4) | 110.4 (4) | Co-C(13)-C(M13) | 121.2 (4) |
| C(T1)-O-B(11) | 126.0 (4) | C(7)-C(13)-B(8) | 109.2 (4) |
| C(T4)-O-B(11) | 123.4 (4) | C(7)-C(13)-C(M13) | 116.9 (4) |
| O-C(T1)-C(T2) | 104.7 (4) | B(8)-C(13)-B(12) | 124.7 (4) |
| C(T1)-C(T2)-C(T3) | 105.3 (5) | B(8)-C(13)-C(M13) | 116.6 (4) |
| C(T2)-C(T3)-C(T4) | 104.8 (5) | B(12)-C(13)-C(M13) | 114.2 (4) |
| O-C(T4)-C(T3) | 102.6 (4) | C(13)-C(M13)-C(E13) | 115.7 (5) |
| C(3)-B(1)-C(7) | 104.0 (4) | Co-C(2′)-C(M2′) | 141.6 (5) |
| B(1)-C(3)-C(M3) | 121.0 (5) | Co-C(2′)-B(7′) | 90.0 (3) |
| B(1)-C(3)-B(8) | 104.8 (4) | C(M2′)-C(2′)-C(3′) | 119.9 (6) |
| C(M3)-C(3)-B(4) | 113.2 (4) | C(M2′)-C(2′)-B(6′) | 127.9 (6) |
| C(M3)-C(3)-B(8) | 120.6 (4) | C(M2′)-C(2′)-B(7′) | 128.4 (5) |
| C(M3)-C(3)-C(9) | 122.2 (4) | C(3′)-C(2′)-B(6′) | 111.1 (5) |
| C(3)-C(M3)-C(E3) | 111.9 (5) | C(2′)-C(M2′)-C(E2′) | 114.4 (7) |
| B(1)-C(7)-C(M7) | 121.7 (5) | Co-C(3′)-C(M3′) | 136.4 (5) |
| B(1)-C(7)-C(13) | 106.9 (4) | Co-C(3′)-B(7′) | 90.4 (3) |
| B(6)-C(7)-C(M7) | 114.9 (5) | C(2′)-C(3′)-C(M3′) | 121.3 (6) |
| C(M7)-C(7)-B(12) | 118.9 (4) | C(2′)-C(3′)-B(4′) | 112.1 (5) |
| C(M7)-C(7)-C(13) | 118.4 (5) | C(M3′)-C(3′)-B(4′) | 125.8 (7) |
| C(7)-C(M7)-C(E7) | 119.0 (6) | C(M3′)-C(3′)-B(7′) | 133.2 (5) |
| C(3)-B(8)-C(13) | 112.0 (5) | C(3′)-C(M3′)-C(E3′) | 113.8 (7) |
| C(9)-B(8)-C(13) | 122.6 (4) | C(3′)-B(4′)-B(5′) | 106.8 (6) |
| Co-C(9)-C(M9) | 121.3 (4) | B(4′)-B(5′)-B(6′) | 102.7 (5) |
| C(3)-C(9)-C(M9) | 115.4 (4) | B(5′)-B(6′)-C(2′) | 107.1 (5) |
| B(4)-C(9)-C(M9) | 116.5 (4) | | |

the recently reported facile conversions of $B_5H_8^-$ to $B_{10}H_{14}$ and of $B_6H_9^-$ to $B_{12}H_{16}$.[14] Thus, routes to ultralarge carborane cages via $(C_2B_4)M(C_4B_8)$ and $(C_4B_8)_2M$ metallacarborane systems seem entirely feasible, and work along these lines continues.

The structural characterization of the mixed-ligand complex **6a** furnishes additional evidence of the reliability and generality of the skeletal electron-counting correlations as embodied in PSEPT. The structures of **6a** and the $(C_4B_8)_2Co$ system described in the preceding paper, together with earlier work,[10-12] demonstrate that the PSEPT approach is valid for cages at least as large as fragments of 14- and 15-vertex polyhedra. As more such structures are revealed, it will be interesting to see just how far the theory correlates with observation in this realm of large boron clusters.

## Experimental Section

**Materials and Instrumentation.** The carboranes $Et_4C_4B_8H_8$ and *nido*-2,3-$Et_2C_2B_4H_6$ were prepared by previously reported methods.[15] Anhydrous iron(II) chloride (Alfa) wa s dried at high temperature in vacuo before use. Other reagents and materials, and the instrumentation employed, were as described in the preceding paper.[1]

**Reaction of $Na^+_2Et_4C_4B_8H_8^{2-}$ with $CoCl_2$ Followed by $Na^+Et_2C_2B_4H_5^-$.** A 100-mL three neck flask was charged with 1040 mg (4 mmol) of $Et_4C_4B_8H_8$ and placed in a liquid-nitrogen bath. Sodium naphthalenide ($NaC_{10}H_8$, 8 mmol in 35 mL of THF) was added, and the mixture was warmed to room temperature, the dark green solution acquiring the yellow color of $Et_4C_4B_8H_8^{2-}$. After the solution was cooled to −63 °C, 1560 mg (12 mmol) of anhydrous $CoCl_2$ was added in vacuo. The mixture was warmed to room temperature and stirred for 2 h, causing it to turn dark brown. After it was cooled in liquid nitrogen, a solution of $Na^+Et_2C_2B_4H_5^-$ (obtained by reaction of 4 mmol of $Et_2C_2B_4H_6$ with 6 mmol of NaH in THF) was introduced to the reactor via filtration in vacuo, and the mixture was again warmed to room temperature and stirred for 2 h, during which the color turned black.

The reaction mixture was exposed to the atmosphere and stirred for 1 h, after which the THF solvent was removed on a rotavaporator and the residue extracted with $CH_2Cl_2$. After removal of the insolubles by filtration, the filtrate was rotavaporated and the residue placed on top

(14) Brewer, C. A.; Grimes, R. N. *J. Am. Chem. Soc.* **1984**, *106*, 2722.

(15) (a) Maynard, R. B.; Grimes, R. N. *Inorg. Synth.* **1983**, *22*, 215. (b) Maynard, R. B.; Borodinsky, L.; Grimes, R. N. *Inorg. Synth.* **1983**, *22*, 211.

of a silica gel column and eluted successively with hexane, 1:1 hexane/$CH_2Cl_2$, and $CH_2Cl_2$, after which all these fractions were combined, the solvent was removed by rotavaporation, and the residue was heated at 50 °C in vacuo to remove naphthalene. The remaining residue was placed on preparative silica TLC plates and eluted with hexane followed by 1:1 hexane/$CH_2Cl_2$. Over 20 bands were observed, most of which were in very small quantity and were not collected. The products isolated and characterized, in order of elution, were as follows. Colorless $Et_6C_6B_{12}H_{12}$ (**8**): yield 10 mg; $R_f$ (hexane) 0.92; mass spectrum (EI) cutoff at $m/e$ 391 (parent, $^{13}C^{12}C_{17}{}^{11}B_{12}{}^{1}H_{42}{}^{+}$, intensity pattern corresponding to $C_{18}B_{12}$). Golden $(Et_4C_4B_8H_7)_2Co_2$ (**2b**): yield 50 mg (0.078 mmol); $R_f$ (hexane/$CH_2Cl_2$) 0.82; identified[1] from its $^{11}B$ NMR spectrum and $R_f$ value. Compound **2b** is completely air stable in both solution and the solid state. Purple $(Et_2C_2B_4H_4)Co(Et_4C_4B_8H_7OC_4H_8)$ (**6a**): yield 80 mg (0.15 mmol); $R_f$ (hexane/$CH_2Cl_2$) 0.52; mp 158 ± 1 °C; high $m/e$ 521 (parent, $^{13}C^{12}C_{21}{}^{11}B_{12}{}^{16}O^{1}H_{49}{}^{59}Co^{+}$, $C_{22}B_{12}OCo$ pattern); $^1H$ NMR ($CDCl_3$; t = triplet, m = multiplet, s = singlet) 0.80 t, 1.02 t, 1.10 t, 1.18 t, 1.40 m, 1.45 t, 1.68 m, 2.00 m, 2.12 s, 2.20 m, 2.40 m, 2.58 m, 2.70 m, 5.08 s. Compound **6a** is completely air stable. Green $(Et_4C_4B_8H_8)_2CoH(OC_4H_8)$ (**3b**): yield 15 mg (0.03 mmol); $R_f$ (hexane/$CH_2Cl_2$) 0.50; mp 82 °C dec; high $m/e$ 653 (parent, $^{13}C^{12}C_{27}{}^{11}B_{16}{}^{16}O^{1}H_{65}{}^{59}Co^{+}$, $C_{28}B_{16}OCo$ pattern); $^1H$ NMR ($CDCl_3$) 0.88 t, 0.97 t, 1.00 t, 1.12 t, 1.25 s, 1.54 s, 2.16 s, 5.21 s, 5.29 s. This compound is not air sensitive but decomposes in vacuo at room temperature and must be stored in a freezer. Orange $(Et_4C_4B_8H_7)_2CoH$ (**4b**): yield (60 mg (0.10 mmol); $R_f$ (hexane/$CH_2Cl_2$) 0.46; mp 86 °C dec; high $m/e$ 579 (parent, $^{13}C^{12}C_{23}{}^{11}B_{16}{}^{1}H_{55}{}^{59}Co^{+}$, $C_{24}B_{16}Co$ pattern); $^1H$ NMR ($CDCl_3$) 0.88 t, 0.98 t, 1.11 t, 1.16 m, 1.25 m, 1.52 s, 2.17 s, 2.38 m, 2.70 m. This compound survives brief exposure to air but exhibits some air sensitivity over long periods (hours).

The product residues remaining on the silica column were eluted with a 1:1:1 mixture of acetone, hexane, and $CH_2Cl_2$, which gave a large red-brown band and two very small bands, which were not characterized. The large band was red-brown $(Et_2C_2B_4H_3)Co(Et_4C_4B_8H_6OC_4H_8)$ (**7**): yield 132 mg (0.26 mmol); $R_f$ (1:1:1 acetone/hexane/$CH_2Cl_2$) 0.51; mp 138 °C dec; high $m/e$ 519 (parent, $^{13}C^{12}C_{21}{}^{11}B_{12}{}^{16}O^{1}H_{47}{}^{59}Co^{+}$, $C_{22}B_{12}OCo$ pattern); $^1H$ NMR (acetone-$d_6$) 1.20 s, 2.05 s, 2.10 s, 2.14 s, 2.60 s, 2.90 s (broad), 3.80 s. Compound **7** is moderately air stable, decomposing slowly (days) in solution.

**Iodination of 6a.** A 40-mg sample of **6a** and 5 mg of $I_2$ were placed in a 50-mL flask, 20 mL of hexane was added, and the mixture was stirred for 1 h, after which $O_2$ was bubbled into the solution for another 1 h. Following removal of solvent by evaporation, the residue was extracted with hexane and developed on a TLC plate. A few milligrams of green $(Et_2C_2B_4H_4)Co(Et_4C_4B_8H_8)(I)(OC_4H_8)$ (**6b**), $R_f$ 0.55, was collected and characterized mass spectroscopically (high $m/e$ 649, parent ion $^{13}C^{12}C_{21}{}^{11}B_{12}{}^{16}O^{127}I^{1}H_{50}{}^{59}Co^{+}$, $C_{22}B_{12}OICo$ pattern, with intense fragments corresponding to $Et_4C_4B_8H_9I^{+}$ and $Et_4C_4B_8H_8OC_4H_8^{+}$). Several other small bands were observed but not collected.

**Reaction of $Na^{+}{}_2Et_4C_4B_8H_8^{2-}$ with $FeCl_2$ Followed by $Na^{+}Et_2C_2B_4H_5^{-}$.** A solution of the disodium salt of $Et_4C_4B_8H_8^{2-}$, prepared from 4 mmol of the neutral carborane as described above, was cooled to −15 °C, and 12 mmol of anhydrous $FeCl_2$ was added in vacuo. The dark green mixture was allowed to warm to room temperature and stirred for 2 h, during which it turned dark brown. A 4-mmol sample of $Na^{+}Et_2C_2B_4H_5^{-}$ in THF, prepared as described above, was added to the mixture, and stirring was continued overnight. The mixture was exposed to the atmosphere, stirred for 30 min, extracted with 1:1 $CH_2Cl_2$/acetone, and filtered through a 3-cm layer of silica. The solvent was removed by evaporation and the residue placed on a silica gel column and eluted with hexane followed by 1:1 hexane/$CH_2Cl_2$ and finally 1:1 acetone/$CH_2Cl_2$. The first band ($R_f$ 0.88 in hexane) was red $(Et_2C_2B_4H_4)(OC_4H_8)Fe(Et_4C_4B_8H_8)$ (**9a**): yield 50 mg; high $m/e$ 519 (parent, $^{13}C^{12}C_{21}{}^{11}B_{12}{}^{16}O^{1}H_{50}{}^{56}Fe^{+}$, $C_{22}B_{12}OFe$ pattern). Band 2 ($R_f$ 0.45 in hexane; 0.69 in 1:1 hexane/$CH_2Cl_2$) was red $(Et_2C_2B_4H_3)FeH_2(Et_4C_4B_8H_7)$ (**10**): yield 25 mg; high $m/e$ 447 (parent, $^{13}C^{12}C_{17}{}^{11}B_{12}{}^{1}H_{42}{}^{56}Fe^{+}$, $C_{18}B_{12}Fe$ pattern). Band 3 ($R_f$ 0.64 in 1:1 hexane/$CH_2Cl_2$) was purplish black **9b**, yield 15 mg (high mass 519, isomeric with **9a**, vide supra; parent envelope similar to that of **9a**, corresponding to a $C_{22}B_{12}OFe$ pattern). Band 4 ($R_f$ 0.65 in 1:1 acetone/$CH_2Cl_2$) was red $(Et_4C_4B_8H_7)FeH(Et_2C_2B_3H_4)$ (**11**): yield 165 mg; high $m/e$ 433 (P − 3, $^{13}C^{12}C_{17}{}^{11}B_{11}{}^{1}H_{39}{}^{56}Fe^{+}$, $C_{18}B_{11}Fe$ pattern).

**X-ray Structure Determination on $(Et_2C_2B_4H_4)Co(Et_4C_4B_8H_7OC_4H_8)$ (6a).** Single crystals of **6a** were grown by slow evaporation from $CH_2Cl_2$ solution, and a selected crystal (0.60 × 0.60 × 0.40 mm) was mounted on a glass capillary and examined by precession photography, from which it was determined to be acceptable for data collection. Table III lists the data collection parameters and crystal data. The cell dimensions and space group were found by standard methods on an Enraf-Nonius CAD-4 diffractometer equipped with a graphite monochromator, and the $\theta$–$2\theta$ scan technique was employed[16] to record the intensities of all nonequivalent reflections for which $1.5° < 2\theta < 53°$. Scan widths were calculated as $A + B \tan \theta$, where $A$ and $B$ are defined as in the accompanying paper[1] and had values of 0.60 and 0.35, respectively. Octants collected were $+h,+k,\pm l$.

The intensities of three standard reflections showed fluctuations no greater than those expected from Poisson statistics. The raw intensity data were corrected for Lorentz–polarization but not for absorption. Of the 4178 independent intensities, there were 2013 with $F_o^2 > 3\sigma(F_o^2)$, where $F_o^2$ was estimated from counting statistics.[17] These data were used in the final refinement of the structural parameters.

A three-dimensional Patterson synthesis was employed to locate the cobalt atom, which in turn allowed the remaining non-hydrogen atom positions to be determined. Full-matrix least-squares refinement was carried out as described elsewhere.[16] The atomic scattering factors for non-hydrogen atoms were taken from Cromer and Waber[18] and those for hydrogen from Stewart et al.[19] The effects of anomalous dispersion for all non-hydrogen atoms were included in $F$ by using the values of Cromer and Ibers[20] for $\Delta F'$ and $\Delta F''$.

Additional Fourier difference functions permitted location of the non-methyl hydrogen atoms, which were included in the refinement for two cycles of least-squares refinement and then held fixed in subsequent cycles.

The model converged with $R = 0.057$ and $R_w = 0.061$. A final Fourier difference map was featureless. Listings of the observed and calculated structure factors, and of calculated thermal parameters, are available (see information on supplementary material).

**Acknowledgment.** The assistance of Dr. T. L. Venable in recording the $^{11}B$ NMR spectra is gratefully acknowledged. This work was supported by the National Science Foundation, Grant No. 81-19936.

**Supplementary Material Available:** Listings of observed and calculated structure factors, anisotropic thermal parameters, and calculated mean planes (18 pages). Ordering information is given on any current masthead page.

(16) Freyberg, D. P.; Mockler, G. M.; Sinn, E. *J. Chem. Soc., Dalton Trans.* **1976**, 447.
(17) Corfield, P. W. R.; Doedens, R. J.; Ibers, J. A. *Inorg. Chem.* **1967**, *6*, 197.
(18) Cromer, D. T.; Waber, J. T. "International Tables for X-ray Crystallography"; Kynoch Press: Birmingham, England, 1974; Vol. IV.
(19) Stewart, R. F.; Davidson, E. R.; Simpson, W. T. *J. Chem. Phys.* **1965**, *42*, 3175.
(20) Cromer, D. T.; Ibers, J. A. In ref 18.